

**Feasibility study of  $e - \mu$  azimuthal correlation  
from open heavy flavor in ALICE at LHC  
energies**

**M.Sc. Thesis**

by

**Jaswant Singh**



**DISCIPLINE OF PHYSICS  
INDIAN INSTITUTE OF TECHNOLOGY INDORE**

**June 2018**

# Feasibility study of $e - \mu$ azimuthal correlation from open heavy flavor in ALICE at LHC energies

A THESIS

*Submitted in partial fulfillment of the  
requirements for the award of the degree*

of

Master of Science

by

Jaswant Singh



DISCIPLINE OF PHYSICS

INDIAN INSTITUTE OF TECHNOLOGY INDORE

June 2018



*DEDICATED*  
*TO*  
*MY FAMILY*

# *Acknowledgements*

---

*I would like to thank my thesis advisor Dr. Ankhi Roy, Department of Physics, Indian Institute of Technology, Indore for giving me his invaluable time, guidance, co-operation and constant encouragement and providing all the necessary facilities throughout the course of my studies and preparation of the manuscript in the present form.*

*Thank you to all my classmates they have always support and encourage me.*

*I would like to thank the expert who was there for my help and I have learned many things since I came in touch with Sudhir Rode and Ankita Goswami.*

*They provided me with unfailing support and continuous encouragement throughout my years of study during thesis writing. Special thanks to Ankita Goswami for valuable guidance and support in thesis work.*

*I would also like to acknowledge Sudhir Rode, Ankita Goswami, Sudeep Ghosh, Sumit Kundu and Ravindra Rathore for their support and all of my M.Sc classmates of Department of Physics, Indian Institute of Technology, Indore.*

*Finally, I would like to convey my heartfelt gratitude and sincere appreciation to Sudhir Rode, Ankita Goswami for being there in any need.*

*(Jaswant Singh)*



# Contents

---

<b>Acknowledgements</b>	<b>v</b>
<b>1 Introduction</b>	<b>1</b>
1.1 Standard Model . . . . .	1
1.2 Quantum Chromodynamics (QCD) . . . . .	3
1.3 Evolution of the System . . . . .	3
1.4 Quark Gluon Plasma (QGP) . . . . .	5
1.4.1 Nuclear modification factors . . . . .	5
1.4.2 $J/\psi$ Suppression . . . . .	6
1.5 Heavy flavor production processes . . . . .	6
1.6 Motivation . . . . .	8
<b>2 Experimental Techniques</b>	<b>11</b>
2.1 ALICE Detector . . . . .	12
2.2 ALICE Layout . . . . .	12
2.2.1 Inner Tracking System . . . . .	13
2.2.2 Time Projection Chamber . . . . .	13
2.2.3 Time of Flight . . . . .	14
2.2.4 Muon Chamber . . . . .	15
2.2.5 A Brief Introduction to Pythia and Root Frame-work . . . . .	15

<b>3</b>	<b>Analysis</b>	<b>17</b>
3.0.1	Analysis in PHENIX . . . . .	17
3.0.2	Analysis in ALICE . . . . .	22
3.0.3	PID in ALICE frame work . . . . .	25
<b>4</b>	<b>Conclusion and Future Outlook</b>	<b>29</b>
	References . . . . .	31

# Figures

---

1.1	Elementary particles and force carriers in standard model. This figure has been taken from [2]. . . . .	2
1.2	Schematic picture of a heavy ion collision. Figure has been taken from [4]. . . . .	3
1.3	Representation of space time evolution [8] . . . . .	4
1.4	Theoretical phase diagram of quark matter as a function of temperature $T$ and baryon chemical potential $\mu$ [3]. . . . .	5
1.5	There are few examples of heavy flavor production. (a,b) Leading order. (c) Pair creation (with gluon emission). (d) Flavour excitation. (e) Gluon splitting. (f) Events classified as gluon splitting but of flavour-excitation character This figure has been taken from [9]. . . . .	7
1.6	Sketch of the possible semi-leptonic decays of a $D\bar{D}$ pair . . . . .	9
1.7	(Color online) Comparison of the measured $p + p$ pair yield [(red) points] with heavy-flavor production in POWHEG ([blue] dashed curve), PYTHIA [(black) solid curve], and MC@NLO [(green) long dashed curve]. The pair $e - \mu$ yield from the subset of PYTHIA events, when the $c\bar{c}$ is not produced at the event vertex, is plotted as the dotted (black) curve. Each Monte Carlo curve was scaled by a single parameter to match the observed yield [11]. . . . .	10
1.8	Rapidity distribution of lepton pairs from the charm and bottom [12]	10
2.1	This figure shows that ring of LHC and from four interaction points there is one ALICE detector [10]. . . . .	11
2.2	Schematic layout of the ALICE detector [15]. . . . .	13
2.3	Schematic picture of TPC (Time projection Chamber) [16] . . . . .	14

3.1	This figure shows that decay of $D^0$ meson. . . . .	18
3.2	These plots show that yield from heavy flavor: Figure(a) like sign $e - \mu$ pairs and (b) unlike-sign $e - \mu$ pairs (c) after subtraction of like the sign from unlike sign left is correlated unlike-sign pairs and (d) plot from PHENIX data . . . . .	20
3.3	Comparison of data with simulation. (a) plots from data and plot (b) from simulation by using PYTHIA 8. . . . .	21
3.4	The distribution of $e - \mu$ pairs follow the Gaussian function. The simulation has been done by PYTHIA8 event generator . . . . .	21
3.5	Invariant production cross-section of charm and bottom . . . . .	23
3.6	Invariant production cross-section of charm and bottom from LO and NLO terms . . . . .	24
3.7	These plots are showing (a) like–sign yield (b) unlike – sign yield (c) correlated unlike – sign pairs at LHC energies $\sqrt{s} = 7$ TeV and $\sqrt{s} = 0.9$ TeV . . . . .	25
3.8	These plots are showing Correlated unlike-sign yield at LHC energies $\sqrt{s} = 0.9$ and $\sqrt{s} = 7$ TeV from open heavy flavor generated by PYTHIA 8 event generator, distribution fitted with a Gaussian function. . . . .	26
3.9	Identification of electron from TPC and TOF . . . . .	27
3.10	The schematic diagram of muon chamber . . . . .	28

# Tables

---

3.1	This table shows that cross-section of different reactions. This is taken from PYTHIA 8 . . . . .	20
3.2	Parameters a,b and c are given . . . . .	22
3.3	Parameters a,b and c are given . . . . .	25

# Chapter 1

---

## Introduction

What are the fundamental particles ? Perhaps answer of this question may be different to different person. But the particle physicist may ask at what energy. In earlier time technology was not so advanced that can create very high energy. One needs high energy accelerator to penetrate more and more inside atoms. Last few decades we have really advanced in accelerator science which helps us to discover many fundamental particles in nature. Those particles were predicted by the standard model as well. In this chapter, first we will discuss about the standard model which is the theory of fundamental forces (except gravitational force) and particles. Next we will introduce Quantum Chromodynamics (QCD) which is the theory of strong interaction as my work is related to the strong force. QGP (Quark Gluon Plasma) which is expected to be formed in the early stages after the big-bang, can be created through heavy ion collisions in the laboratory. So, QGP and different observables to know about this state of the matter will be explained next. Heavy flavor (charm and bottom) quarks are created in the early stages of the heavy ion collision, can be the carrier of the information about the QGP medium. Finally, in this chapter we will focus on heavy flavour mesons and its production processes as my thesis work is based on the open heavy flavour mesons.

### 1.1 Standard Model

Theories and discoveries since 1930s resulted in providing prodigious insights into the fundamental structure of matter. The strive to explain the fundamental properties of matter leads to the theory of standard model. It was

presented by Glashow, Salam and Wienberg in 1970. The standard model is very reach in explaining experimental results with very high accuracy. According to the standard model, elementary particles can be classified into 6 quarks, 6 leptons, 4 gauge bosons and Higgs boson, unearthed short time ago . Each family of quarks and leptons can be subdivided into generations. Six quarks are paired into three generations: the up ( $u$ ) and down ( $d$ ) quarks are from the first generation; the charm ( $c$ ) and strange ( $s$ ) are from the second generation; and the top ( $\tau$ ) and bottom ( $b$ ) are the third generation. Similar to quarks, the leptons are also arranged into three generations: the electron ( $e$ ) and electron neutrino ( $\nu_e$ ); the muon ( $\mu$ ) and muon neutrino ( $\nu_\mu$ ); the tau ( $\tau$ ) and tau neutrino ( $\nu_\tau$ ) [1]. Each quarks and leptons also have their corresponding anti-particle. Any force working in the universe can be classified as one of the fundamental forces. These fundamental forces are: electromagnetic force, strong force, weak force and gravitational force. Electromagnetic force carrier is photons( $\gamma$ ), strong force carrier is gluons ( $g$ ), weak force carrier are  $W^\mp, Z^0$  and gravitational force carrier is graviton. Among four forces, gravitational is very frail force which is not counted in particle physics. Except gravitational force, other three forces are explained by the standard model. This Figure 1.1 shows all elementary particles and force carriers

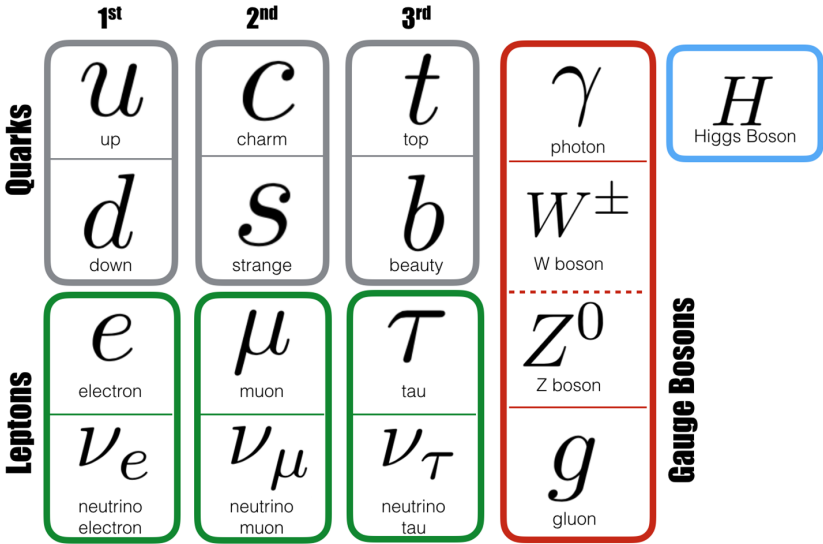


**Figure 1.1.** Elementary particles and force carriers in standard model. This figure has been taken from [2].

## 1.2 Quantum Chromodynamics (QCD)

Atoms are made of nucleus and surrounded by electrons. Nucleus is made of proton and neutron, they also called as nucleons. Protons and neutrons are made of quarks and gluons. Quarks are bind by strong force which is carried by gluons. Quantum Chromodynamics is theory of strong force. There are two peculiar properties of this force: quark confinement, asymptotic freedom. Quarks can not freely exist due to color confinement, they are confined inside hadrons. Mesons are one type of hadron which are made of one quark and One anti-quark. Baryons are those particles which are made of three quarks. When quarks are very close to each other they behave like a free particles and if one tries to separate quarks from each other inside nucleon they feel strong force. This is known as quark confinement.

## 1.3 Evolution of the System

In a heavy ion collision experiment two heavy nuclei collide at relativistic velocities. Due to very high velocity they are Lorentz contracted along the direction of motion and come into view like a almond shape. After the smashing of two incoming beam of particles, the system is evolved, all the different scene are shown in Figure 1.2. The collision at the interaction point  $t=0, z=0$ . Space time evolution of the system after the collision is shown in Figure 1.3,

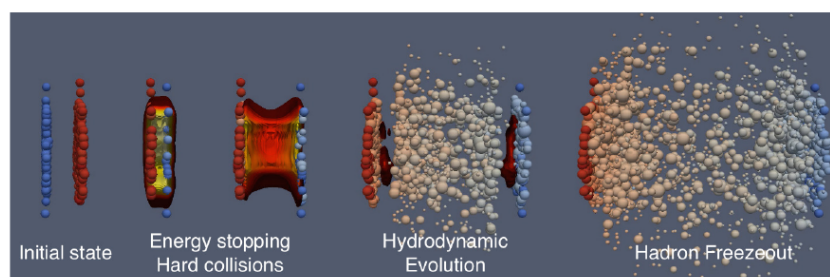


**Figure 1.2.** Schematic picture of a heavy ion collision. Figure has been taken from [4].

after the collision of heavy particles at very high energy. Whole energy are deposited in a very small region. Colliding particles have quarks and gluons,

after the collision quark and gluon medium is formed. The energy density at the collision center is sufficiently high and it can form a strongly interacting matter consisting of deconfined quarks and gluons, called quark gluon plasma (QGP). This medium is locally equilibrium and after a small time medium will expand due to pressure gradient. Temperature will go down and Hadronization will starts. Hadronization is a process in which hadron are formed after the collision. The corresponding temperature is called the critical temperature ( $T_c$ ). As the temperature of the system falls below a freeze out temperature called chemical freeze out temperature ( $T_{ch}$ ), the inelastic collision among the constituents ceases. At this moment the chemical composition of the produced particles get fixed. After the chemical freeze out the ingredient can interact among themselves via elastic scattering which may further change the shape of their transverse momentum spectra. When the mean free path of the hadrons outdo the dynamical size of the system, the elastic interaction among the hadrons conclude. This is called kinetic freeze out and the corresponding temperature is known as kinetic freeze out temperature ( $T_{fo}$ ). After that the hadrons streamline freely to the detector and get detected by the detector.

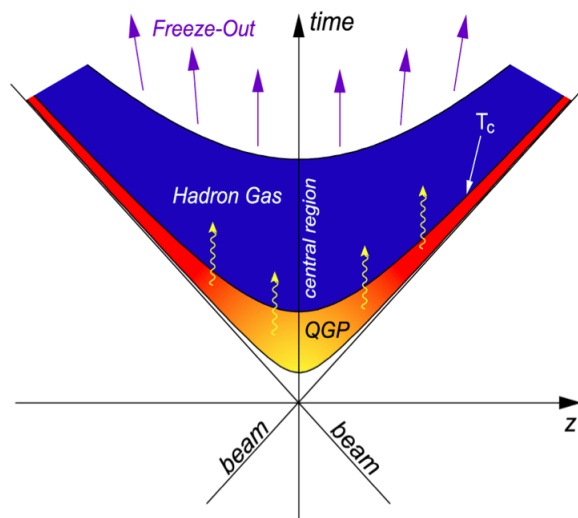


**Figure 1.3.** Representation of space time evolution [8] .

## 1.4 Quark Gluon Plasma (QGP)

The phase diagram for QCD matter is not known precisely, but an estimate of it is shown in figure 1.4. At sufficiently high temperature and/or density the system transformed into the deconfined state, known as a quark gluon plasma (QGP). QGP is a state of matter which contains quarks and gluons in the deconfined state. This state can not be measured directly due to very small time. Particles created after the collision can, carry information about the medium that is created at the interaction point. There are some signature of QGP : Jet quenching, Nuclear modification factors,  $J/\psi$  Suppression, Strangeness enhancement are some the signatures of known about the QGP.

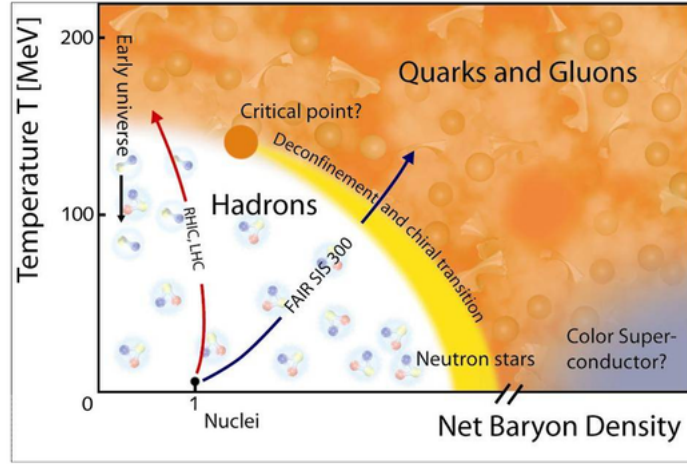


**Figure 1.4.** Theoretical phase diagram of quark matter as a function of temperature  $T$  and baryon chemical potential  $\mu$  [3].

In this thesis nuclear modification factor and  $J/\psi$  suppression will be discussed.

### 1.4.1 Nuclear modification factors

QGP can be studied by introducing the nuclear modification factor  $R_{AA}(p_T)$ , given by

$$R_{AA}(p_T) = \frac{dN/dp_T|_{AA}}{\langle N_{coll} \rangle dN/dp_T|_{pp}}$$

Where ratio of particle production yield of nucleus-nucleus  $dN/dpt_{AA}$  to pp collision which is scaled by the binary nucleon – nucleon collision. Any change in particle production in nucleus nucleus collision will be expressed by  $R_{AA}(p_T)$ . The hadron production may be reduced is due to energy loss as the hadrons cross the QGP. If this ratio is unity may be their is no production of QGP at given energy otherwise  $R_{AA}(p_T)$  will , deviate from unity. The evaluation of heavy flavor quark yield in heavy ion collisions provides important information concerning energy loss at a partonic scale which in turn can provide information about the produced QCD matter. Heavy quarks are primarily produced in initial hard scattering processes, making them good probes since they undergo the entire evolution of the created QCD matter.

### 1.4.2 $J/\psi$ Suppression

$J/\psi$  is a bound state of  $c\bar{c}$  quarks. The quarkoniums (or bottomoniums) are the bound states of quark anti-quark pairs like  $c\bar{c}$ (or  $b\bar{b}$ ). They are created in the early stages of the collision. The production of  $J/\psi$  is suppressed in heavy ion relative to pp collision. If QGP is formed, then  $J/\psi$  formation is suppressed due to color screening potential. In QGP, color charge of quarks are screened, by Debye Screening. So that  $c\bar{c}$  pairs is not able to formed.

## 1.5 Heavy flavor production processes

There are few processes involved in the production of heavy flavor (Heavy flavor means charm and beauty). These processes are explained - Production of heavy flavor are divided in three processes: Pair creation, Gluon splitting, Gluon fusion. The production of heavy flavor and which process is dominating depending on the energy of the colliding hadron. The explanation is given below of all processes:

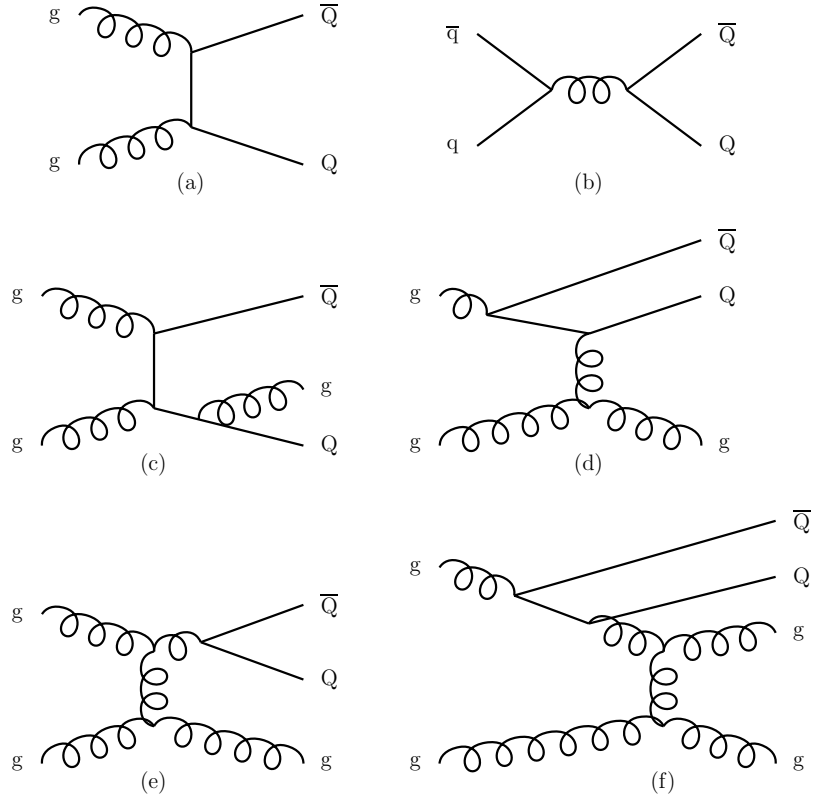


**Figure 1.5.** These are a few examples of heavy flavor production. (a,b) Leading order. (c) Pair creation (with gluon emission). (d) Flavour excitation. (e) Gluon splitting. (f) Events classified as gluon splitting but of flavour-excitation character. This figure has been taken from [9].

## Pair Creation

Pair creation is the LO process (Leading order) and processes include  $q\bar{q} \rightarrow Q\bar{Q}$  and  $g\bar{g} \rightarrow Q\bar{Q}$ . Because anti-quarks are less abundant than gluons inside the nucleus, the gluon fusion process is dominant. This will produce charm pairs that are back-to-back in azimuthal angle. Gluon radiation can occur in either the initial or final state, but this will shift the kinematics of the process rather than change the rate.

## Flavor Excitation

Flavor excitation is an NLO (Next-to-Leading-Order) effect, involving processes  $Qg \rightarrow Qg$  and  $Qq \rightarrow Qq$ . This involves a heavy quark being put on its mass shell by a parton in the other beam, which means a heavy quark

already has to be present before the interaction takes place. It is generally created through a gluon splitting process,  $g \rightarrow Q\bar{Q}$ , so the total interaction is effectively  $gq \rightarrow Q\bar{Q}q$  or  $gq \rightarrow Q\bar{Q}g$ . Heavy flavor distributions vanish for  $2 < m_Q^2$ , so the virtuality must be greater than  $m_Q^2$  for this process to occur. One heavy quark is involved in the hard scattering vertex [9].

## Gluon Splitting

Gluon splitting means a gluon is split into a heavy quark and ant-quark(heavy). Gluon splitting process is  $gg \rightarrow gQ\bar{Q}$  in either the initial or final state. There is no heavy flavor is participated in the hard scattering. The gluon splitting occur in the final state, since in the initial state the time-like gluon is restricted to have smaller virtuality. Where  $q$  and  $Q$  are light and heavy quark respectively.

## 1.6 Motivation

Feasibility study of  $e - \mu$  azimuthal correlation from open heavy flavor in  $pp$  collisions at LHC energies is reported in this thesis. Open heavy flavor hadron is any hadron that contains one heavy flavour (charm ( $c$ ) or Beauty ( $b$ )) and other is any light quarks or anti-quarks depending on whether it is meson or baryon. Heavy flavors which have very high bare mass, are created in early stages of the collisions via initial hard scattering. Gluon fusion is the most dominant process by which the heavy flavours are produced. This makes charm production an important probe of the initial gluon structure function [5]. In heavy ion collisions, the study of heavy quark energy loss is a good probe of the medium. This is because the energy loss is proportional to the broadening in  $p_T$ , which depends on the properties of the medium [6]. The previous measurements of charm semi-leptonic decays have been done using  $e^+ e^-$  and  $\mu^+ \mu^-$  pairs. However, these are subject to charge correlated backgrounds such as thermal production, Drell-Yan processes, and resonance decay. Because these processes produce opposite sign pairs of the same lepton species, the  $e - \mu$  measurement is spared from these backgrounds, making this a

clean measurement of charm [7]. The major remaining source of background is the pairing of uncorrelated electrons and muons, but these can be removed by a like-sign subtraction. We have chosen to study the  $e - \mu$  azimuthal angular separation because charm pairs are expected to be produced back-to-back. Therefore their decay products are expected to have an angular separation of  $\pi$  on average. This will give a clearer signal than studying the invariant mass spectrum, which has no well-defined peak for this type of decay. The study of

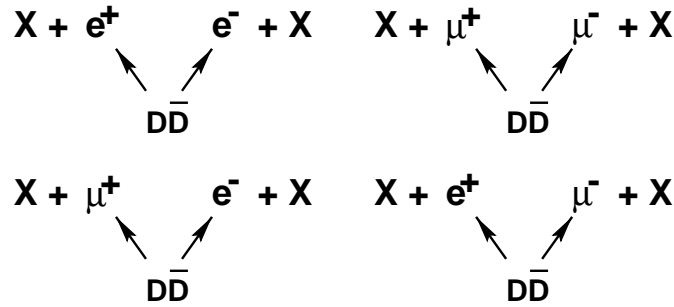


**Figure 1.6.** Sketch of the possible semi-leptonic decays of a  $D\bar{D}$  pair

azimuthal correlation of  $e - \mu$  from heavy flavour at RHIC energy  $\sqrt{s} = 200$  GeV was done by the PHENIX collaboration which is shown in Fig:1.7. At RHIC energy  $\sqrt{s} = 200$  GeV, LO processes are dominating in the production of charm but NLO process are also contributing but less.

As we know LHC has collected a huge data set at very high energy (e.g  $\sqrt{s} = 0.9$  TeV, 2.76 TeV, 5.5 TeV, 13 TeV). So, this is a very good opportunity to analyse the  $e - \mu$  correlation at LHC with ALICE setup. As PHENIX analysis is having very statistical error, we are expect less statistical error at LHC. Also we observe how the higher order process are contributing at LHC energies. So for large statistics we have done feasibility study of electro-muon correlation from open heavy flavor at LHC energies in ALICE setup. In ALICE acceptance we can study of  $e - \mu$  correlation in different rapidity region as shown in figure 1.8. Rapidity distribution of  $e - \mu$  pairs connect the mid and forward rapidity region.

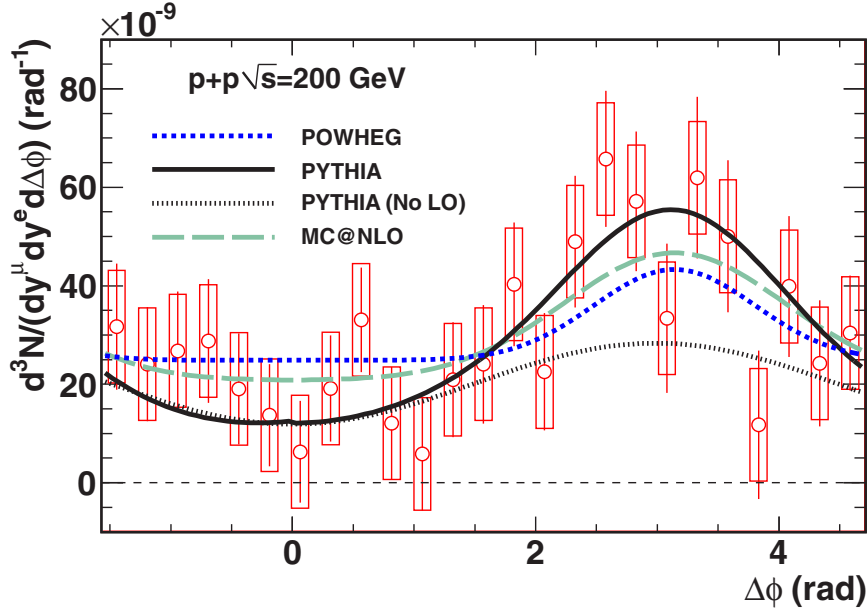


**Figure 1.7.** (Color online) Comparison of the measured  $p + p$  pair yield [(red) points] with heavy-flavor production in POWHEG [(blue) dashed curve], PYTHIA [(black) solid curve], and MC@NLO [(green) long dashed curve]. The pair  $e - \mu$  yield from the subset of PYTHIA events, when the  $c\bar{c}$  is not produced at the event vertex, is plotted as the dotted (black) curve. Each Monte Carlo curve was scaled by a single parameter to match the observed yield [11].

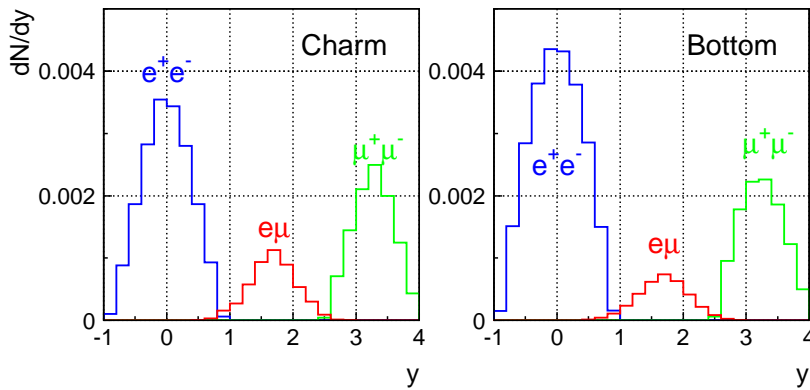


**Figure 1.8.** Rapidity distribution of lepton pairs from the charm and bottom [12]

## Chapter 2

# Experimental Techniques

Large Hadron collider is the largest heavy ion collider in the world which is established in the Geneva and it consists of a super conducting ring having radius 27 km [13] as shown in Figure 2.1.

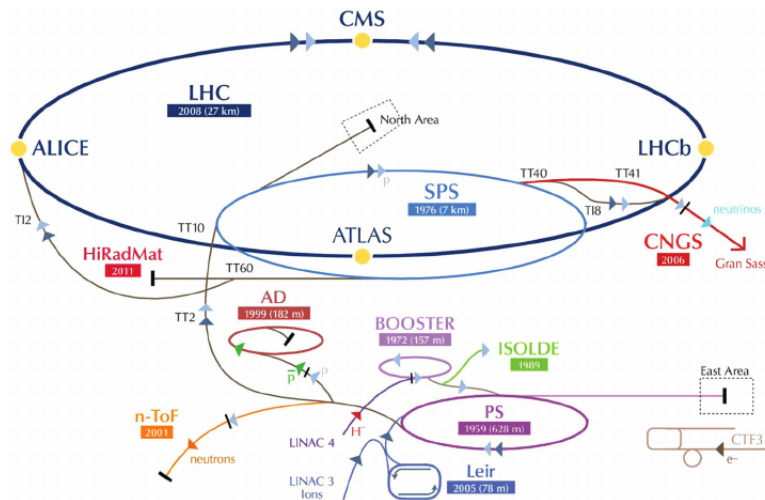


**Figure 2.1.** This figure shows that ring of LHC and from four interaction points there is one ALICE detector [10].

When two ions collide at very high energies the whole energy is deposited in very small region which is utilized to produce the particles. Since the available energy is greater in the collider as compare to fixed target experiment, collider is preferred as compare to fixed target experiment. Now question is "what type of particle can be accelerated?" Only charge particles can be accelerated in the LHC. Suppose if we choose electron for collider, when electron is moving in orbit with so much high velocity there will be large loss of energies in the form of radiation known as synchrotron radiation, so light charge particle is not

suitable. The acceleration of heavy ions is suitable because of low synchrotron radiation energy loss [14].

After the collision, the produced particles should be detected which is a big task for the physicists. They are using different detector for detecting particles. The track which passes through magnetic field itself contains a great deal of information as the curvature of the tracks indicates the charge, momentum is directly proportional to the radius of curvature. However, in order to detect these observables it is required to have some sort of detector. In this chapter, we have discussed some of the ALICE detector which were used to detect  $e$  and  $\mu$ , also the ROOT frame-work and PYTHIA 8 event generator. We have tried to the feasibility study using PYTHIA 8 event generator with ROOT frame-work.

## 2.1 ALICE Detector

ALICE(A Large Ion Collider Experiment) is a detector specialized in measuring and analyzing heavy-ion collisions. ALICE is able to detect charge particles ( $e^\pm$ ,  $\pi^\pm$ ,  $\mu^\pm$ ) and neutral (e.g  $\gamma$ ) particle.

## 2.2 ALICE Layout

How does detector work? if someone asks you how to get information about something. Your answer like that first of all you have to interact with that thing about which you want the information. This is the way of getting information about an object. The same thing applies here if we want the information about the particles produced in the collision we have to make those particles interact with the material in the detector. All particles deposit their information in the detector medium and associated electronic with detector medium will give the all deposited information in the form of signal. Here some sub-detectors are discussed below: Inner Tracking System(ITS), Time of Flight(TOF), Time projection chamber(TPC), Muon Chamber.

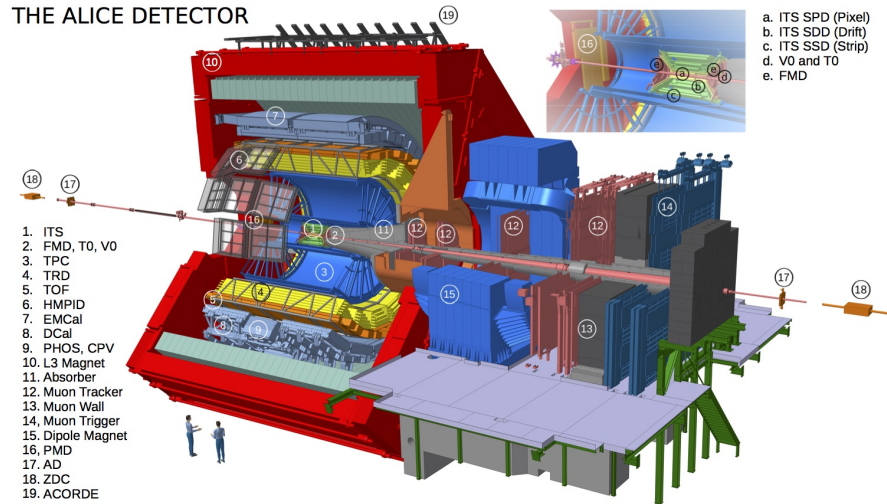


**Figure 2.2.** Schematic layout of the ALICE detector [15].

## 2.2.1 Inner Tracking System

ITS is a sub-detector which is placed around the beam pipe. It consists of silicon. It has six layers, each one is cylindrical in shape with radius from 4.00 cm to 43.00 cm around the beam pipe. It is used to determine the track and collision vertex. In heavy ion collisions at high energy, there is difficulty to resolve the tracks due to high track density near the beam pipe. That is why the first two layers of the ITS which is called as Silicon Pixel Detectors (SPD) has the very high resolution. Also, there are two layers of Silicon Drift Detectors (SDD) in the middle and two outer most layers of Silicon micro-Strip Detectors (SSD) which has relatively low resolution since the track density decreases. The main task of SPD is to determine the primary vertex position. Last two SDD and SSD detector are used to identify the particle identification by their energy deposition and also for tracking purpose.

## 2.2.2 Time Projection Chamber

The primary task of TPC is to measure the particle momentum, particle identification. TPC covers full azimuthal range and phase space range is  $|\eta| = 1.8$  and 500 cm in length.

TPC is a very good tracking detector with low material budget and it is

also called as heart of the ALICE detector.

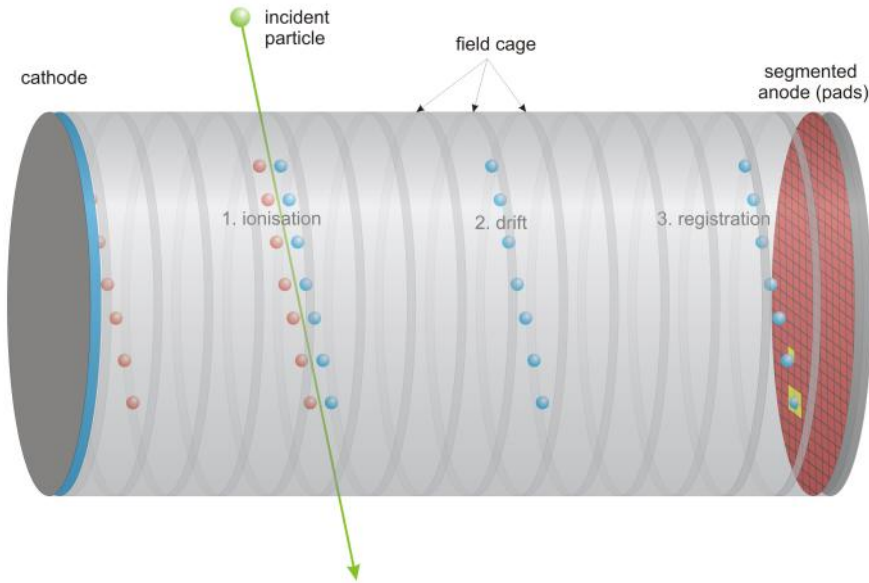


**Figure 2.3.** Schematic picture of TPC (Time projection Chamber) [16]

TPC is cylindrical in shape with inner and outer radius 0.85m and 2.85m respectively. TPC is a gas detector with central high electric field is applied in TPC. When particle entered in chamber they ionized the gas and they will drift towards the opposite potential electrodes. Choice of a gas for detector is not random, one has to take care of stability, ageing and radiation length.

### 2.2.3 Time of Flight

The TOF is a gas based Multigap Resistive Plate Chamber (MRPC) and kept at 2.70 m to 3.99 m (acceptance  $\eta < 0.9$ ) at polar angle  $45^\circ$  to  $135^\circ$ . Two different particles with same momentum can be identified by time of flight technique within the time resolution of the TOF which is about 80 ps. A particle with mass  $m$  and momentum  $p$  having velocity is

$$\beta = p / \sqrt{p^2 + m^2} \quad (2.1)$$

For a path length  $L$  the time of flight is inversely proportional to its velocity  $\beta$  :

$$T = \frac{L}{c\beta} \quad (2.2)$$

Two particles have same momentum but different mass have different time of flight

$$T_1 - T_2 = \frac{L}{c} \left( \sqrt{1 + \frac{m_1^2}{p^2}} - \sqrt{1 + \frac{m_2^2}{p^2}} \right) \quad (2.3)$$

## 2.2.4 Muon Chamber

Main task of muon spectrometer is measure the open heavy flavor production and quarkonia production by muonic channel. The muon spectrometer works in the pseudo-rapidity  $-4 < \eta < -2.5$  corresponding to angular range  $171^\circ - 178^\circ$ . At LHC energies muon produced from semi-leptonic charm and beauty decay are dominated so it is identify the muon particles. Muon spectrometer is combination of front absorber, tracking system, dipole magnet, muon filter, beam shield and trigger chambers. Photons and hadrons that are coming toward the muon spectrometer particles will interact with absorber and lose their energy. Absorber is separate muons from other particles and it is remove the low energy background [17].

## 2.2.5 A Brief Introduction to Pythia and Root Frame-work

PYTHIA 8 is a  $C++$  based event generator which is broadly used in experimental high energies physics for the simulation. Currently in PYTHIA available program is  $pp$ ,  $p\bar{p}$ ,  $e^+e^-$  and  $\mu^+\mu^-$  incoming beam. PYTHIA is main class we can extract all information about the all process from this main class [18].

```
Pythia pythia;
pythia.readString("HardQCD:all = on");
pythia.readString("PhaseSpace:pTHatMin = 20.");
```

```
pythia.readString("Beams:eCM = 7000.");  
pythia.init();
```

These are the pythia setting that we used. And connect with ROOT Frame work with root library to take the root files. There are also more setting like PDF (parton density function) etc.

## Root Frame-work

Root is a frame-work to Analyze the observations. Comparison of observations with theoretical is a standard work in HEP(high energy physics). ROOT frame work is very easy to use. Let see how we use root as for different work and ROOT is C++ based software [19].

1. As a function plotter.
2. one can plots measurements.
3. Histogram can also make.

For the beginners there is a directory "root/tutorial/" can also learn root with help of tutorial macors. But for any person that want to learn ROOT frame work, should knows very good understanding of C++ language.

# Chapter 3

---

## Analysis

In this chapter, we mainly discuss the  $e - \mu$  azimuthal correlation from the heavy flavor at RHIC(Relativistic Heavy Ion Collision ) and LHC (Large Hadron Collider) energies at PHENIX (Pioneering High Energy Nuclear Interaction eXperiment) and ALICE(A Large Ion Collider Experiment) experiment respectively.The reaction is

$$p + p \rightarrow c\bar{c} + X \rightarrow e^{\pm}\mu^{\mp} + X$$

Where the opposite sign electron pair is from the  $c\bar{c}$  pair decay. The electrons and muons decay from open heavy flavor is depicted in Figure 3.1. First we have tried to reproduce PHENIX work, Heavy-flavor electron-muon correlations in  $p + p$  collisions at  $\sqrt{s} = 200$  GeV with the help of PYTHIA 8 event generator. In this analysis, at RHIC energy only leading order processes are involved but there is very less contribution of NLO processes. We are going to do the same simulation for LHC energies. At higher energies, maybe the next to leading order processes are also participate in the production of heavy flavor.

### 3.0.1 Analysis in PHENIX

#### Electron Identification

The electron is identified by the use of electromagnetic calorimeter (EMCal) which is made of the atoms that have the high atomic number. Due to a field of electrons and nucleus of the material, an original electron will accelerate or

de-accelerate and produce radiation. The produced radiation convert into the electron and positron. That pair production and photons lead to an electromagnetic shower that is detected by EMCal in PHENIX detector. The position of EMCal in PHENIX detector is  $|\eta| < 0.5$ . Electrons are identify with transverse momentum  $p_T > 0.5 \text{ GeV}/c$ . Because of that signal to background ratio is very small so that they have applied the  $p_T$  cut.

## Muon Identification

The muon is identified by muon detector. In the PHENIX detector, muon detector is placed at the end of all detectors, muons are produced with the very high momentum they will interact weakly with the material. And to remove the background some absorber are place in front of muon detector. At the end of the detector, trigger system is placed which ensure about the muons. The acceptance of muon detector in PHENIX detector for eta coverage is  $1.2 < |\eta| < 2.4$ .  $P_T > 1.0 \text{ GeV}/c$  Here  $p_T$  cut applied to remove the background.

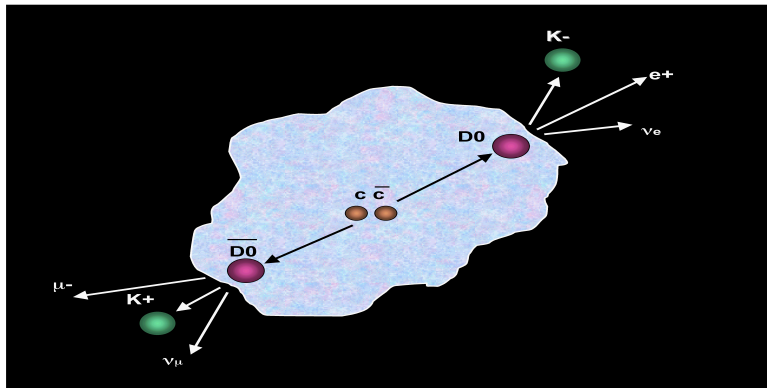


**Figure 3.1.** This figure shows that decay of  $D^0$  meson.

## Background Subtraction

Electrons and muons are come from light and heavy flavor decay and from misidentified hadrons. The total number of pairs is equal to the sum of an electron-muon pair from the heavy flavor, correlating a heavy flavor decay

product with a light flavor decay and from the heavy flavor. The all electron-muon yield can be written as

$$N^{e\mu}(\Delta\Phi) = N_H^{e\mu}(\Delta\Phi) + N_{LH}^{e\mu}(\Delta\Phi) + N_L^{e\mu}(\Delta\Phi) \quad (3.1)$$

$N_H^{e\mu}(\Delta\Phi)$  Total number of pair of Electron-muon from all sources.  $N_{LH}^{e\mu}(\Delta\Phi)$  Total number of pair from heavy flavor decay.  $N_L^{e\mu}(\Delta\Phi)$  yield from correlating a heavy flavor decay product with light flavor decay.  $N_L^{e\mu}(\Delta\Phi)$  yield from light hadron decay. The equation can be break like and unlike-sign terms.

$$N_{like}^{e\mu}(\Delta\Phi) = N_{LH,unlike}^{e\mu}(\Delta\Phi) + N_{L,unlike}^{e\mu}(\Delta\Phi) \quad (3.2)$$

$$N_{unlike}^{e\mu}(\Delta\Phi) = N_{H,unlike}^{e\mu}(\Delta\Phi) + N_{LH,unlike}^{e\mu}(\Delta\Phi) + N_{L,like}^{e\mu}(\Delta\Phi) \quad (3.3)$$

There are few assumptions –

$$N_{like}^{e\mu}(\Delta\Phi) = N_{L,unlike}^{e\mu}(\Delta\Phi) \quad (3.4)$$

$$N_{LH,like}^{e\mu}(\Delta\Phi) = N_{LH,unlike}^{e\mu}(\Delta\Phi) \quad (3.5)$$

The heavy flavor  $e - \mu$  signal distribution is the difference between the unlike-sign and like-sign inclusive correlation :

$$N_H^{e\mu}(\Delta\Phi) = N_{unlike}^{e\mu}(\Delta\Phi) - N_{like}^{e\mu}(\Delta\Phi) \quad (3.6)$$

## Simulation

In  $p + p$  collision at PHENIX experiment at  $\sqrt{s} = 200$  GeV, the like-sign ( $e^- - \mu^-$ ,  $e^+ - \mu^+$ ) pairs as shown in figure 3.2 (a) from all the sources of electrons and muons, unlike-sign ( $e^- - \mu^+$ ,  $e^+ - \mu^-$ ) pairs from all sources as shown in figure 3.2(b). By using the subtraction method, subtract the like-sign yield from unlike-sign yield, however, finally we get correlated unlike-sign yield which is only from the open heavy flavor. It will give a signal at  $\pi$ . At RHIC energy only leading order (LO) is dominating due to which  $e - \mu$

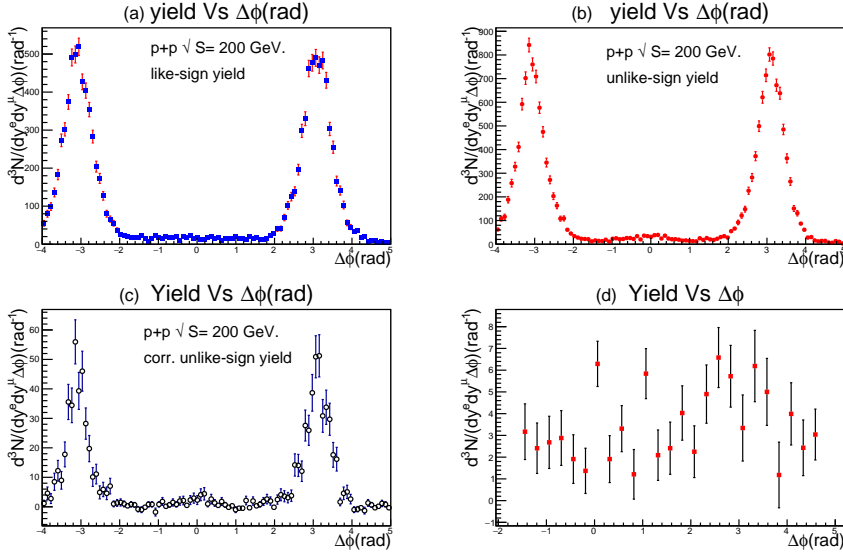


**Figure 3.2.** These plots show that yield from heavy flavor: Figure(a) like sign  $e - \mu$  pairs and (b) unlike-sign  $e - \mu$  pairs (c) after subtraction of like the sign from unlike sign left is correlated unlike-sign pairs and (d) plot from PHENIX data

pairs created but NLO terms are participating with very less contribution. In the production of charm the reaction  $gg \rightarrow c\bar{c}$  is more participating because of interaction cross-section is more. The interaction cross-section is given below in the table 3.1 of different reactions. From this reaction cross-section, one can estimate which reaction is dominating.

**Table 3.1.** This table shows that cross-section of different reactions. This is taken from PYTHIA 8

Process code	Reaction	cross-section ( $\sigma \mu b$ )
121	$gg \rightarrow c\bar{c}$	0.127
122	$q\bar{q} \rightarrow c\bar{c}$	0.064
123	$gg \rightarrow b\bar{b}$	0.109
124	$q\bar{q} \rightarrow b\bar{b}$	0.055

### Correlated $e - \mu$ unlike sign Yield Distribution

The distribution of  $e - \mu$  pairs from open heavy flavor follow the Gaussian distribution. The distribution, fitting with Gaussian function as shown in Figure 3.4. The  $e - \mu$  yield follow the Gaussian function, the function is given

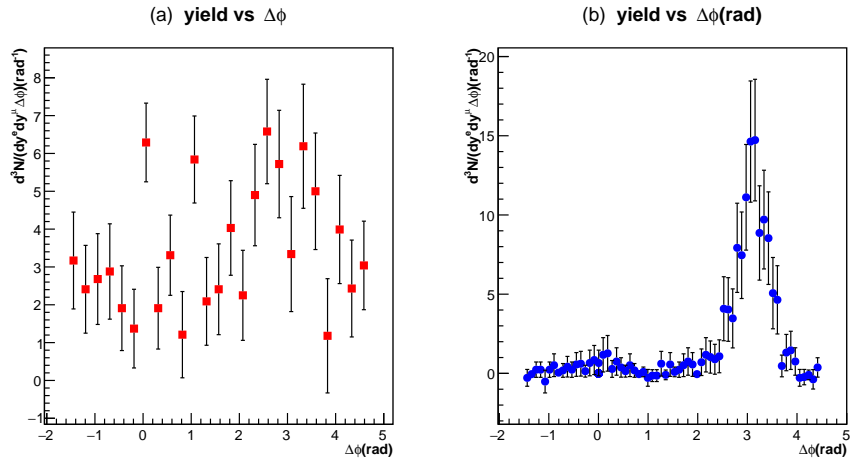


**Figure 3.3.** Comparison of data with simulation. (a) plots from data and plot (b) from simulation by using PYTHIA 8.

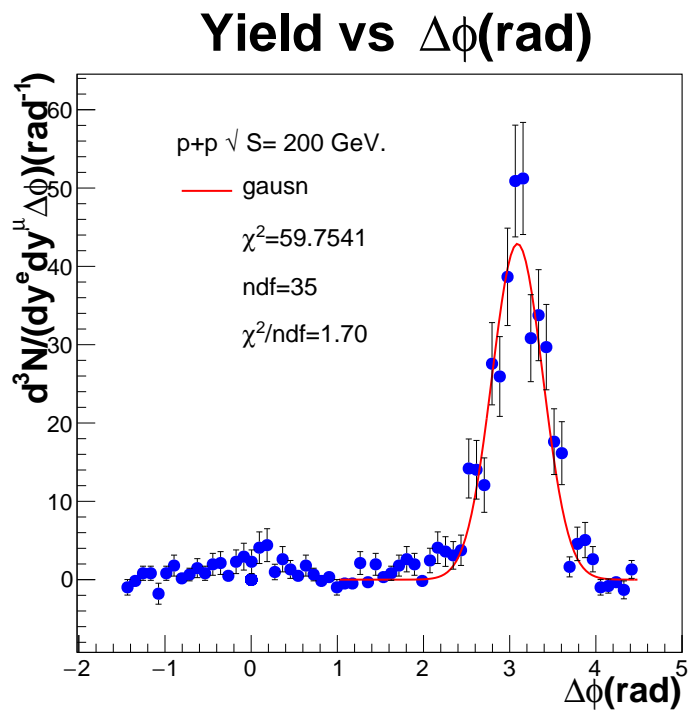


**Figure 3.4.** The distribution of  $e - \mu$  pairs follow the Gaussian function. The simulation has been done by PYTHIA8 event generator .

as

$$f(x) = \frac{a}{c\sqrt{2\pi}} \exp \left[ -\frac{1}{2} \left( \frac{x-b}{c} \right)^2 \right] \quad (3.7)$$

Where a,b and c are parameters. The values of these parameters are given in the Table 3.2.

$\frac{\chi^2}{NDF} = 1.70$  where  $\chi^2 = 59.7541$ , NDF=35 (number of degree of freedom).

There is only contribution of leading order at RHIC energy at  $\sqrt{s}=200$  Gev.

Parameters	Parameters value $\pm$ errors
a	$31.697 \pm 1.69$
b	$3.09 \pm 0.01$
c	$0.29 \pm 0.01$

**Table 3.2.** Parameters a,b and c are given

From the data figure 3.3(d) one can not estimate about the background so we have tried to fit simulation with data to understand the background. After the fitting with Gaussian function, the mean value ( $3.09 \pm 0.01$ ) tells that back to back decay of D meson at  $\Delta\Phi = \pi$ . The width of ( $0.29 \pm 0.14$ ) Gaussian function tells about the production of charm.

### 3.0.2 Analysis in ALICE

p + p collision in PHENIX at energy  $\sqrt{s}=200$  GeV simulation has been done by PYTHIA 8 showing that only LO terms are dominating but there is very less contribution of NLO. We want to see what will happen when one goes to higher energies and What extent of NLO contribution in the production of heavy flavor at higher energies.

## Invariant Production Cross-Section of electrons from Charm and Bottom

Now as one goes to higher energies the other terms are also contributing such as Next to leading order terms gluon splitting and Flavor excitation is also contributing in charm and bottom production. From these plots 3.5 one can say

that production probability of charm and bottom is increased as goes to higher energies. The comparison of production of charm and bottom at different energies given in Figure:3.5 At low  $p_T$  more number of particles are produced. As goes to higher  $p_T$ , particles production are decaying exponentially. We discussed NLO terms are also contributing to heavy flavor production in Figure:3.6 and will discuss now azimuthal correlation of  $e - \mu$  at LHC energies in ALICE experiment from the open heavy flavor. As one goes to higher energies NLO processes are also significant. From Fig:3.6 still now LO order are dominate at energies  $\sqrt{s}= 2.76$  and  $\sqrt{s}=5.5$  TeV as compare to NLO.

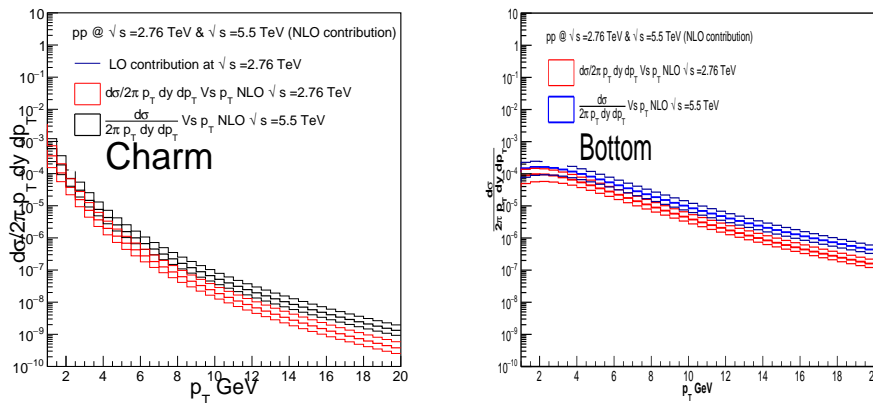


**Figure 3.5.** Invariant production cross-section of charm and bottom .

## Simulation

The simulation has been done by PYTHIA 8 stand alone in ALICE acceptance. As we seen from the PHENIX experiment at  $\sqrt{s}= 200$  GeV only LO terms are contributing. But at higher energies NLO terms are also contributing as shown in figure 3.6. As shown in figure 3.7 (a) like-sign yield and (b) unlike-sign yield from all sources. figure 3.7 (c) correlated unlike-sign yield from open heavy flavor after removing the background by using the subtraction method which is discussed in previous section. he  $D$  and  $\bar{D}$  mesons are made from  $c$  and  $\bar{c}$  together with light quark and anti-quark.  $D$  and  $\bar{D}$  are kinematically correlated but they decay in their individually decay mode. The unlike-sign electrons and muons pairs from  $D$  and  $\bar{D}$  are correlated pairs. Only correlated  $e - \mu$  unlike sign pairs are give a peak at  $\Delta\Phi = \pi$ .

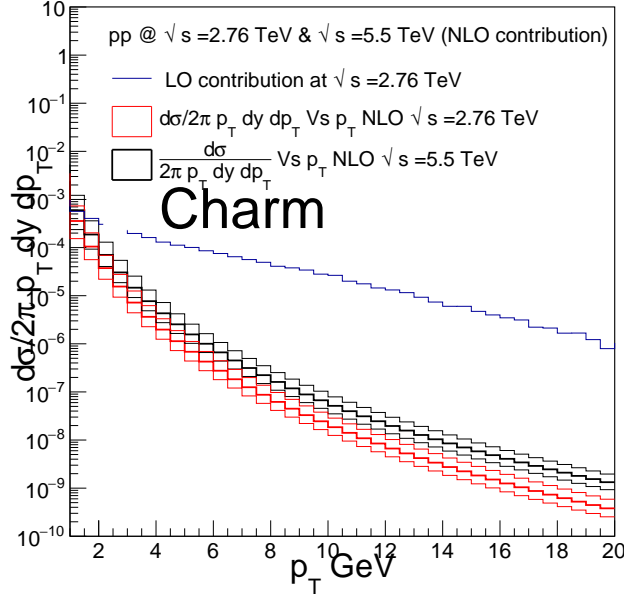


**Figure 3.6.** Invariant production cross-section of charm and bottom from LO and NLO terms .

## Correlated $e - \mu$ unlike-sign Yield Distribution

As we found from the subtraction method only correlated unlike-sign pairs give a peak at  $\pi$ . Same as in ALICE experiment, correlated  $e - \mu$  pairs give a peak at  $\pi$ . Correlated  $e - \mu$  pairs follow the Gaussian as shown in figure 3.8

Fitting function is-

$$f(x) = \frac{a}{c\sqrt{2\pi}} \exp \left[ -\frac{1}{2} \left( \frac{x-b}{c} \right)^2 \right]$$

$$\frac{\chi^2}{ndf} = 1.707 \quad \text{For figure 3.8a}$$

$$\frac{\chi^2}{ndf} = 1.33 \quad \text{For figure 3.8b}$$

where  $\frac{\chi^2}{ndf}$  fitting parameter of function.

The parameters of this distribution is given in a Table 3.3 Width of Gaussian function due the non back to back decay of D meson. The width of the Gaussian function gives us a information of charm production.

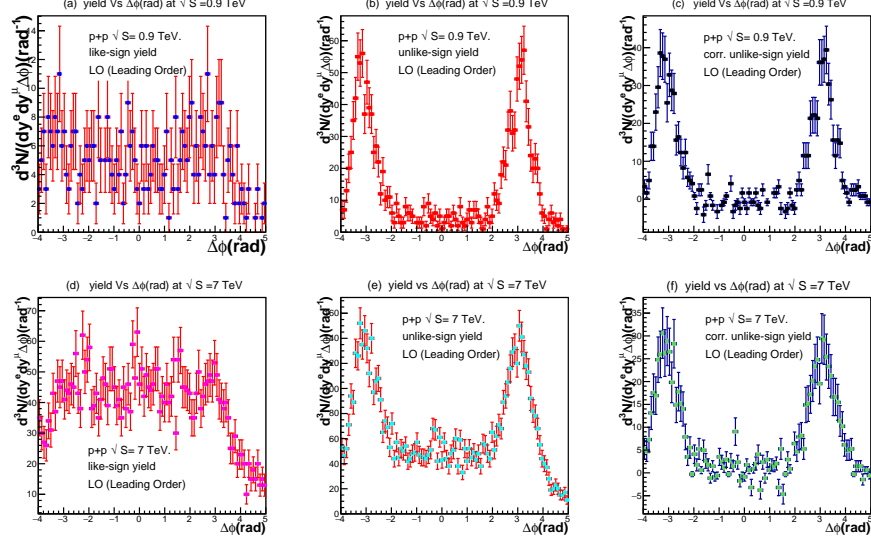


**Figure 3.7.** These plots are showing (a) like–sign yield (b) unlike – sign yield (c) correlated unlike – sign pairs at LHC energies  $\sqrt{s} = 7$  TeV and  $\sqrt{s} = 0.9$  TeV

Parameters	at $\sqrt{s} = 0.9$ TeV	at $\sqrt{s} = 7$ TeV
a	$34.54 \pm 1.77$	$33.53 \pm 1.75$
b	$3.048 \pm 0.049$	$3.08 \pm 0.02$
c	$0.466 \pm 0.044$	$0.49 \pm 0.01$

**Table 3.3.** Parameters a,b and c are given

### 3.0.3 PID in ALICE frame work

Detection of particles is very tedious work. No one cannot detect the particle with the direct way so we need to interact by the indirect way. Because of no one able to see them so that to detect the particles need to first interact with that. Then one takes the help of detector which is made of different materials, by using it, easy to detect particles. The particles first interact with the used material then particles deposited their energy into the material and associated electronic give the information of particles. So here discuss only the identification of electron and muon. Electron and muon are detected by TPC and muon chamber respectively.

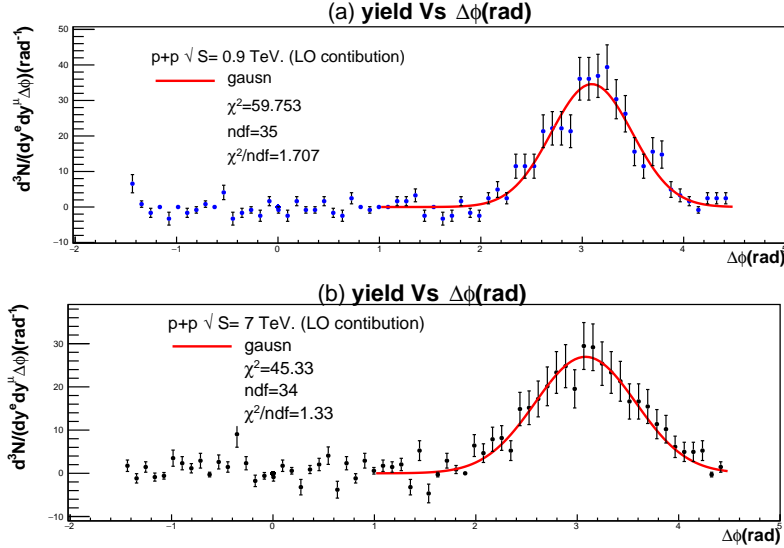


**Figure 3.8.** These plots are showing Correlated unlike-sign yield at LHC energies  $\sqrt{s}=0.9$  and  $\sqrt{s}=7$  TeV from open heavy flavor generated by PYTHIA 8 event generator, distribution fitted with a Gaussian function.

## Identification of Electron from TOF and TPC

By using Bathe-Bloch formula one can detect particle which is tell about energy loss per unit length in the material. The formula given by -

$$-\frac{dE}{dx} = 2\pi N_a r_e^2 m_e c^2 \rho \frac{Z}{A} \frac{z^2}{\beta^2} \left[ \ln \left( \frac{2m_e \gamma^2 v^2 W_{max}}{I^2} \right) - 2\beta^2 - \delta - 2\frac{C}{Z} \right]$$

Where  $r_e$  classical electron radius,  $m_e$  electron mass,  $N_a$  Avogadro's number,  $I$ : mean excitation potential,  $Z$  atomic number of absorbing material,  $A$ : atom weight of absorbing material,  $\rho$  density of absorbing material,  $z$  charge of incident particle in units of  $e$ ,  $\beta = v/c$  of the incident particle,  $\gamma = 1/\sqrt{1 - \beta^2}$ ,  $\delta$  density correction,  $C$  shell correction,  $W_{max}$  maximum energy transfer in a single collision. From the TPC, deposited energies by particle will ionize the gas and create Ion-pairs that collected by the opposite electrode. And give the information about particle. Specific ionization energy loss of the particles when passed through the gas in TPC. Left figure from the TPC and right figure by using TOF. By using TOF we remove the contamination and identify the electron. we have applied following cut to identify the electron-

- **No. of TPC clusters  $\geq 100$**

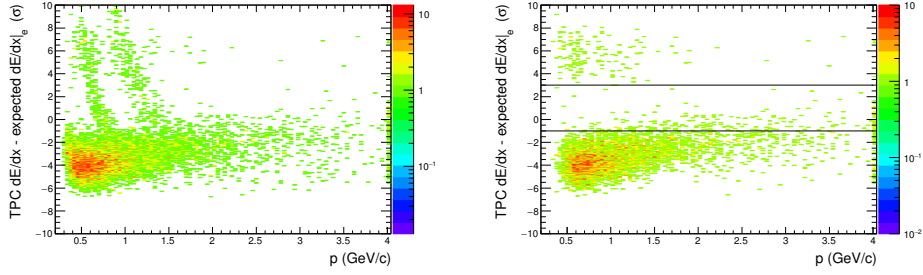


**Figure 3.9.** Identification of electron from TPC and TOF

- No. of TPC  $\frac{dE}{dX}$  clusters (PID)  $\geq 80$
- TOF  $t - \langle \text{TOF } t \rangle_{el} \rightarrow -3 \text{ to } 3 \sigma$
- TPC  $\frac{dE}{dX} - \langle \text{TPC } \frac{dE}{dX} \rangle_{el} \rightarrow -1 \text{ to } 3 \sigma$
- Number of ITS hits  $\geq 4$
- DCA to the primary vertex in xy  $< 1 \text{ cm}$
- DCA to the primary vertex in z  $< 2 \text{ cm}$

One can use all cuts but we have used only first four cuts because of low statistics.

## Identification of Muon from muon chamber

Muons are identified by muon chamber. The first absorber absorbs all particles except muons. Then particles pass through the tracking system in the magnetic field and again pass through the absorber and then finally we get the muons in the trigger system. The schematic figure of muon chamber Fig:3.10

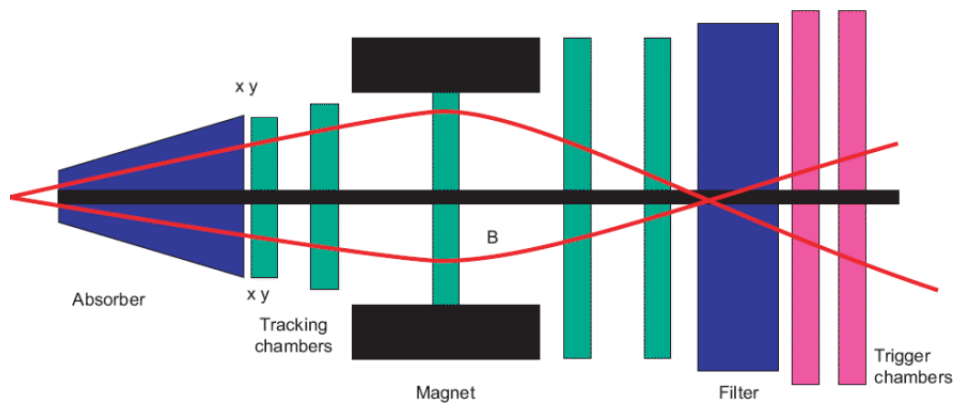


**Figure 3.10.** The schematic diagram of muon chamber

## Conclusion and Future Outlook

The main aim of this thesis was to address the study of the azimuthal correlations of  $e - \mu$  pairs from open heavy flavor from PYTHIA 8 generated  $p + p$  collisions at LHC energies in ALICE experiment. Here we have used the background subtraction method to remove the backgrounds and the electrons, muons that are coming from the light flavor and from other sources. The azimuthal correlation of electrons and muons from open heavy flavor is very useful probe because there is no contribution of more background like Drell-Yan process, Dalitz Decay, Resonance Decay and photon conversion. This azimuthal relation between  $e - \mu$  from the decay of open heavy flavor gives the peak at  $\Delta\Phi = \pi$ . The distribution of  $e - \mu$  pairs follows the Gaussian function. That distribution actually tells us about the production of charm and bottom produced in the  $p + p$  collision. At RHIC energies at  $\sqrt{s} = 200$  GeV only dominating part is LO (Leading Order process). As one goes to higher energies, the NLO (Next to Leading order) terms also starts to contribute to the production of charm. We have identified the electron by using TOF and TPC. We can also find out the ratio of production of charm and bottom. In this thesis we have done simulation for LO processes by PYTHIA 8. So one can do similar simulation by using MC@NLO to see the effect of NLO in the production of charm and bottom.



# Bibliography

---

- [1] David J.Griffiths, Introduction to elementary particles, Wiley publication (2008). [2](#)
  
- [2] [https://www.google.com/search/standard model](https://www.google.com/search/standard%20model) [ix](#), [2](#)
  
- [3] [https://www.google.com/search/qcdphase diagram](https://www.google.com/search/qcdphase%20diagram) [ix](#), [5](#)
  
- [4] Models and Data Analysis Initiative (MADAI) <https://madai-public.cs.unc.edu/> [ix](#), [3](#)
  
- [5] Z. W. Lin and M. Gyulassy, Phys. Rev. Lett. 77, 1222 (1996) doi:10.1103/PhysRevLett.77.1222 [nucl-th/9510041]. [8](#)
  
- [6] M. Golam Mustafa, D. Pal and D. Kumar Srivastava, [8](#)  
Phys. Rev. C 57, 889 (1998) Erratum: [Phys. Rev. C 57, 3499 (1998)] doi:10.1103/PhysRevC.57.3499, 10.1103/PhysRevC.57.889 [nucl-th/9706001].
  
- [7] S. Gavin, P. L. McGaughey, P. V. Ruuskanen and R. Vogt, [9](#)  
Phys. Rev. C 54, 2606 (1996) doi:10.1103/PhysRevC.54.2606 [hep-ph/9604369].
  
- [8] [https://www.google.com/search/space time evolution](https://www.google.com/search/space%20time%20evolution) [ix](#), [4](#)
  
- [9] E. Norrbin and T. Sjostrand, [ix](#), [7](#), [8](#)  
Eur. Phys. J. C 17, 137 (2000) doi:10.1007/s100520000460 [hep-ph/0005110].
  
- [10] [https://home.cern/topics/large – hadron – collider](https://home.cern/topics/large-hadron-collider). [ix](#), [11](#)

- [11] A. Adare et al. [PHENIX Collaboration], Phys. Rev. C 89, no. 3, 034915 (2014) doi:10.1103/PhysRevC.89.034915 [arXiv:1311.1427 [nucl-ex]].
- [12] P. Crochet [ALICE Collaboration], ALICE-INT-2000-01, CERN-ALICE-INT-2000-01.
- [13] Ramona Vogt, Ultrarelativistic Heavy-Ion Collisions, Elsevier (2007).
- [14] Dr. William R. Leo, Techniques for Nuclear and Particle Physics Experiments: A How-to Approach, Springer-Verlag (1987). ix, 10
- [15] [https://en.wikipedia.org/wiki/ALICE\\_experiment](https://en.wikipedia.org/wiki/ALICE_experiment) ix, 10
- [16] <https://indico.ihep.ac.cn/event/3825/contribution/10/material/slides/0.pdf>  
11
- [17] G. Martinez [ALICE Collaboration], Nucl. Phys. A 749, 313 (2005) doi:10.1016/j.nuclphysa.2004.12.059 [hep-ex/0410061]. 12
- [18] <http://home.thep.lu.se/torbjorn/Pythia.html>
- [19] <https://root.cern.ch/>
- ix, 13
- ix, 14